MICRON-IMAGE TRANSFER SYSTEM WITH BRIGHTNESS AMPLIFIER IN GOLD-VAPOR LASER

P. A. Bokhan, T. Ya. Dubnishcheva, D. E. Zakrevskii, and Yu. V. Nastaushev

Institute of Semiconductor Physics, Siberian Division of the Russian Academy of Sciences, Novosibirsk 630090, Russia.

Abstract

A gas-discharge gold-vapor laser on self-terminating transitions with operating wavelength $\lambda = 312.2$ nm has been used to develop a highly efficient system for image transfer. An optical scheme and all its parameters have been chosen optimal for image quality. It has been found both theoretically and experimentally that the best results on micron-structure image transfer are obtained with 2–5-times image reduction. Various types of masks have been used. A 1-μm structure has been resolved due to the choice of optimal exposure time of 10 ms under a period of pulse repetition (0.6 – 0.8) ms; in this case, the minimal fringe dimension was $\sim$2 μm with an image dimension of 2 mm for a laser tube 1.8 cm in diameter.

1. Introduction

The improvement of microlithography as a collection of methods of form-shaping in integrated circuit layers is considered a key problem in microelectronics technology [1]. Progress in lithography concerns both the improvement of traditional optical lithography, including the use of lasers, and the development of new methods. The most important among them are lithography of the far ultraviolet range, x-ray microlithography using synchrotron radiation, and electron-beam and ion-beam lithography.

In this paper, we study the capability, in principle, of the application of optical brightness amplifiers in the UV spectral region using a pulsed gold-vapor laser, $\lambda = 312$ nm. As is known [2], the high gain in pulsed lasers on self-terminating transitions of metal vapor (for example, copper) allows one to project onto the screen a thousand times enlarged image of objects. In this case the light load on the investigated object is several orders of magnitude lower than in traditional projection systems. The brightness amplifier scheme proposed in this work is opposite to the scheme of the projection microscope in a certain sense. Its usage in the manufacturing of integrated circuits can be justified for the following reasons:

1. Diminishing of the light load to the mask as in the projection microscope. This will allow one to lower the cost of the mask on the one hand, and, on the other hand, to accelerate the manufacturing of integrated circuits.

2. The possibility of developing a technological line in which the manufactured integrated circuit is situated in a superhigh-vacuum volume and the mask is outside. This facilitates the system service and lowers its cost.

Translated from a manuscript of the Lebedev Physical Institute, Russian Academy of Sciences.

1071-2836/95/1602-0164$12.50

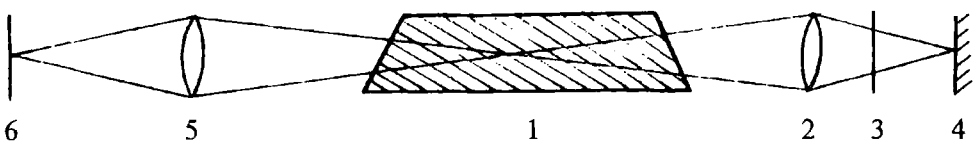

Figure 1. Optical scheme with brightness amplifier for micron-image transfer.

2. Estimate of the Resolving Power of a Brightness Amplifier System with Gold-Vapor Laser

Consider the image-transfer scheme with brightness amplifier presented in Fig. 1. Spontaneous emission (operating wavelength λ) coming from active medium *1* through objective *2* (focal length f_1) illuminates the mask *3*. After the reflection from mirror *4* and the second pass through the mask *3*, the emission comes again into the active medium *1*, which operates now as an amplifier. With the aid of optical system *5*, a multiply amplified signal is projected to the screen *6*, where a shadow picture of the mask *3* appears. A standard pattern is drawn onto the mask *3*, which is made of transparent material. Therefore, the resolution power of such a system W is restricted by the wavelength of emission which is capable of penetrating through a solid-state substance, and for the substrate, $W \simeq 0.12$ μm. If the mask pattern possesses the reflection property, then its projection is possible without mirror *4*. In this case the light reflects from the mask and goes in an opposite direction from screen *6*, i.e., this restriction is not a key one and can be removed by using two variants of one scheme.

It is obvious that the limiting factor of the chosen scheme is the emission linewidth. The use of lens optics leads to aberrations due to the nonmonochromaticity of the emission, and, of course, diminishes the resolution power of the whole system to a certain degree. For the majority of gas lasers the linewidth is small: $\Delta\lambda \simeq 0.1$ cm^{-1}.

We used gold-vapor laser with tube diameters $D_1 = 2$ cm and $D_2 = 2.7$ cm, and lengths $L_1 = 80$ cm and $L_2 = 50$ cm, respectively. The laser with a tube diameter $D_1 = 2$ cm was described in [3]. The laser with a tube diameter $D_2 = 2.7$ cm was supplied with an additional heater [4], and this made it possible to change the pumping regime in a wide range. In particular, it was possible to carry out the excitation by a pulse zug with duration from 10^{-2} to 10^1 s. A mixture of He + Au + H_2 under a hydrogen pressure of 10^{-1} Torr was used in both lasers. An admixture of hydrogen (similar to the copper-vapor laser [5, 6]) and use of the gold red line laser [4] substantially increases the optimal pulse repetition rate and the average output power. Thus, for the tube with diameter $D_2 = 2.7$ cm, P_{av} increases up to 5 times, and reaches $P_{av} \simeq 100$ mW.

Let us estimate the resolution power of such a scheme. As is known, the ultimate angle resolution power ϕ is determined via the diameter of the objective D_0 and the emission wavelength λ, and the number of resolved elements N is determined as $N = D_n/\phi L$, where D_n and L are the diameter and the length of the amplifier tube. For $D_0 = D_n = D$, the number of resolved elements $N = D^2/1.22\lambda L$, i.e., $D = \sqrt{1.22\lambda N L}$. For $\lambda = 312.2$ nm and $D_1 = 2$ cm, $L_1 = 80$ cm, $N_1 = 1300$, and for $D_2 = 2.7$ cm, $L_2 = 50$ cm, $N_2 = 3700$. Consequently, to obtain a submicron image $W < 1$ μm for the image diameter we have $D_{i1} < 1.3$ μm, $D_{i2} < 3.7$ μm. If the image transfer takes place in the whole aperture of the amplifier, one can roughly estimate the maximal number of resolved elements $N_{\max}$. Thus, one can expect simultaneous transfer of about 10^6 elements with the use of the proposed projection system ($N_{\max} = \pi D^4/S_1$) : $N^{(1)}_{\max} \simeq 10^6$, $N^{(2)}_{\max} \simeq 10^7$.

The influence of laser wavelength variation on the parameters of the output optical signal is determined by dispersion of the optical elements and by the diffraction effects. To estimate the value of such distortions

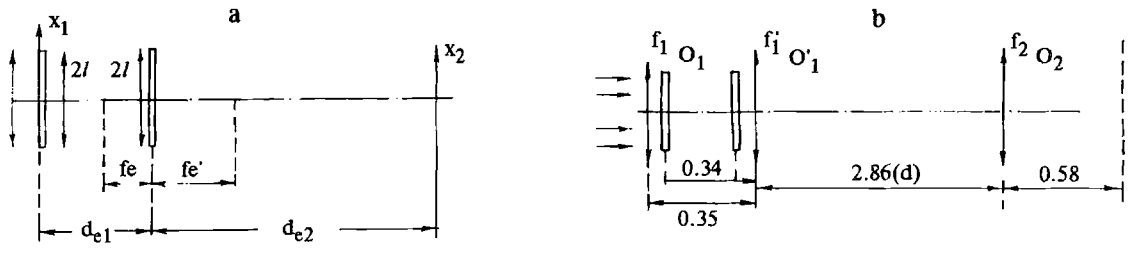

Figure 2. **a)** Optical scheme with equivalent lens; **b)** Simplified equivalent scheme for estimation of line-width influence.

let us consider an equivalent scheme of the optical system shown in Fig. 1. We should stress that the optical beam passes two times through the lens with focal length f_1, i.e., it is convenient to introduce one more lens with focal length $f_1' = f_1$. For our estimations we shall use the geometrical optics approach.

We reduce the optical system to an equivalent lens (see Fig. 2a). The focal length of the equivalent lens f_e and the linear magnification v_e of the equivalent system is determined by formulas [8, 9]:

$$f_e = \frac{f_1 f_2}{f_1 + f_2 - d}; \quad v = \frac{f_1 f_2}{f_1 f_2 - \Delta y}. \tag{1}$$

Here the optical interval Δ is determined as $\Delta = d - f_1 - f_2$, y is the distance between the object and the front focus, $y = 0.34 - f_1$. By substituting numerical values for the real system, one can obtain all the parameters of an equivalent scheme. For this scheme, we may write the condition of conjugation of an object and output planes: $Q_e = d_{e1}^{-1} + d_{e2}^{-1} - f_e^{-1} = 0$. Here $d_{e2}/d_{e1} = v$, $d_{e1} = f_e(1 + v^{-1})$, which is correct for the geometrical optics approximation of thin lenses: $s_i = d_{ei}$. From the equivalent lens it is convenient to pass to a more suitable form of the scheme, which is presented in Fig. 2b. The output plane is the image plane of a transparent X_2, and the equivalent lens has an aperture with dimension $2l$. To take into account the finite aperture, we have introduced as usual a rectangular function

$$\mathrm{rect}\left(\frac{x}{2l}\right) = \begin{cases} 1, & -l \le x \le l, \\ 0, & x > l, x < -l. \end{cases}$$

Let us assume that the lens has no aberrations and forms a real image, and the illumination is nearly monochromatic. This restriction means that the image-forming system is a linear one with respect to the complex amplitude of the field. We shall make calculations by the method of Fourier transform optics following [10-12]. The field $U_i(x_i; y_i)$ at a distance d behind the lens is determined by a complex field $U_0(x_0; y_0)$ behind the object,

$$U_i(x_i; y_i) = \int_{-\infty}^{\infty}\int h(x_i, y_i; x_0, y_0) V_0(x_0, y_0) dx_0 dy_0, \tag{2}$$

where $h(x_i, y_i; x_0, y_0)$ is the amplitude at the point (x_i, y_i) of the field produced by the unit amplitude point source located at the point (x_0, y_0) of the object. Thus, the properties of the imaging system will be completely described if it is possible to determine a pulsed response h. Assuming that the relations obtained for Fresnel diffraction are valid under light propagation at a distance d_i, one can find the pulsed response of the equivalent system (the reaction in the output plane X_2 upon the pulsed disturbance in the plane X_1),

$$h(x_2; x_1) = (\lambda^2 s_1 s_2)^{-1} \exp\left(j\frac{x_1^2 k}{2s_1}\right) \exp\left(j\frac{x_2^2 k}{2s_2}\right) \int_{\infty}^{\infty} \mathrm{rect}\left(\frac{x}{2l}\right) \exp\left(j\frac{kQx^2}{2}\right) \exp\left[-jk\left(\frac{x_1}{s_1} + \frac{x_2}{s_2}\right)x\right] dx. \tag{3}$$

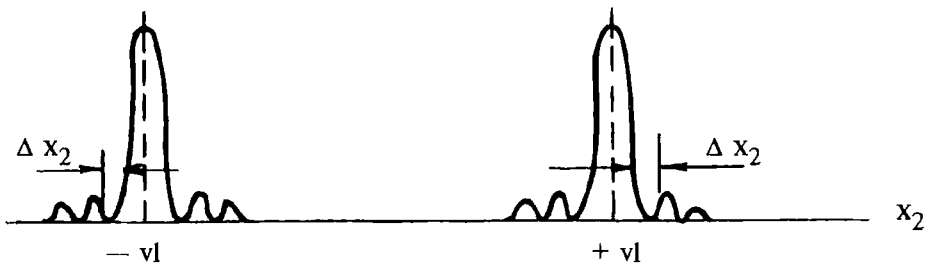

Figure 3. Structure of the image obtained in the optical scheme under investigation.

It is seen that $Q_e = 0$, and

$$h(x_2; x_1) \cong \frac{2l}{\lambda^2 s_1 s_2} \exp\left(j\frac{x_1^2 k}{2s_1}\right) \exp\left(j\frac{kx_2^2}{2s_2}\right) \operatorname{sinc}\left[kl\left(\frac{x_1}{s_1} + \frac{x_2}{s_2}\right)\right], \tag{4}$$

where sinc(x) = sin(x)/x.

We consider the incoming field in the plane of transparent X_1 to be of unit amplitude and

$$U(x_1) = \exp\left(-j\frac{kx_1^2}{2f_1}\right) \operatorname{rect}\left(\frac{x_1}{2l}\right). \tag{5}$$

Here the quadratic phase factor takes into account the influence of lens Q_1. The field in the output plane is

$$U(x_2) = \int_{-\infty}^{\infty} U(x_1) h(x_2; x_1) dx_1. \tag{6}$$

Carrying out all the substitutions and estimating the integral by the stationary phase method, we obtain

$$U(x_2) \cong \frac{As_1}{jkl(1 - s_1/f_1)} \exp\left[j\frac{kl^2}{2s_1}\left(1 - \frac{s_1}{f_1}\right)\right] \left\{\operatorname{sinc}\left[\frac{kl}{s_1}(l + \frac{x_2}{v})\right] + \operatorname{sinc}\left[-\frac{kl}{s_1}\left(l - \frac{x_2}{v}\right)\right]\right\}.$$

Here we took into account for $k/s_i \gg 1$, $A = \dfrac{2l}{\lambda^2 s_1 s_2} \exp\left(j\dfrac{kx_2^2}{2s_2}\right)$. Passing to the intensity, we find with an accuracy of a constant multiple

$$|U(x_2)|^2 \cong B\left\{\operatorname{sinc}^2\left[\frac{kl}{s_1}\left(l + \frac{x_2}{v}\right)\right] + \operatorname{sinc}^2\left[-\frac{kl}{s_1}\left(l - \frac{x_2}{v}\right)\right] + 2\operatorname{sinc}\left[\frac{kl}{s_1}\left(l + \frac{x_2}{v}\right)\right] \operatorname{sinc}\left[-\frac{kl}{s_1}\left(l - \frac{x_2}{v}\right)\right]\right\}. \tag{7}$$

The structure of the image obtained is presented in Fig. 3. The dimension of the image is $2vl = L$, and, because of the diffraction on the transparent boundary, it is changed by a value equal to the doubled distance between the center of the corresponding function sinc(x) and its first zero:

$$\frac{kl}{s_1}\left(l - \frac{\Delta x_2}{v}\right) = -\pi; \quad L = 2lv\left(1 + \frac{\lambda}{2l^2 s_1}\right).$$

Since the transparent dimension change is determined by the diffraction phenomena, the dispersion properties of lens *1*, and the variation of the line width of the laser emission, we obtain for the maximum length change

$$\delta L = |2lv|\delta f_1 + |s_2 l^{-1}|\delta\lambda + |\lambda s_2 l^{-1}|\delta f_1. \tag{8}$$

The formula obtained allows one to estimate the variation of transparent dimensions under conditions of a particular experiment.

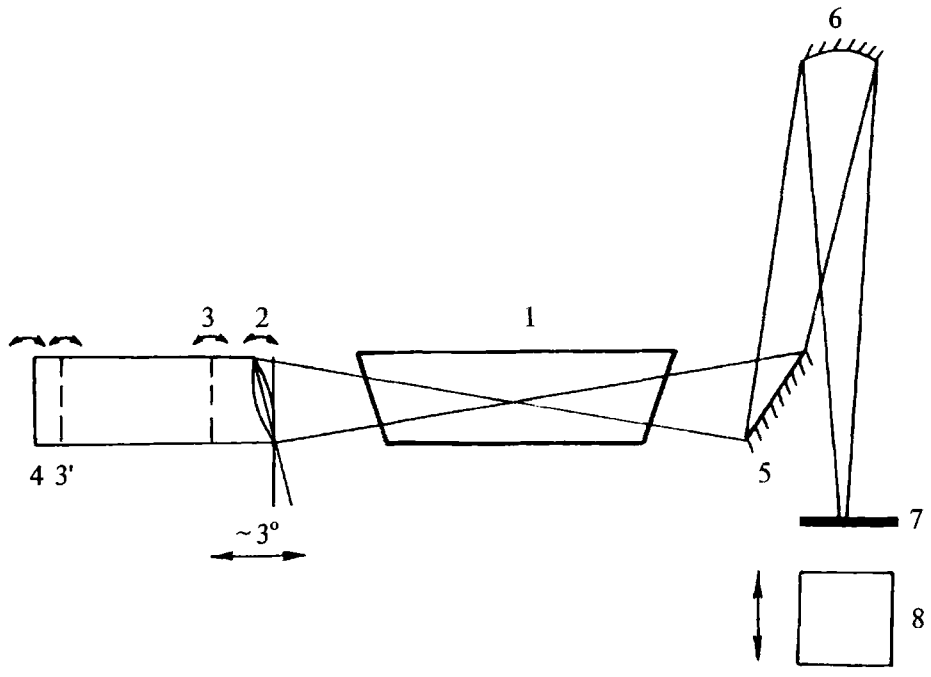

Figure 4. Scheme of a real experiment on micron-image transfer.

3. Micron-Structure Image-Transfer Experiment Using Gold-Vapor Laser

The scheme of a real experiment is given in Fig. 4. An emission with wavelength $\lambda = 312.2$ nm from amplifier *1* through objective *2* with focal distance f_1 illuminates mask *3* under negative projecting, or 3′ under positive projecting. After reflection from mirror *4* in the first case, or from mask 3′ in the second one, the emission is amplified by amplifier *1* and falls onto folding mirror *5*, and then onto a concave mirror *6* with focal distance f_2. As a result, the image of mask *3* appears in the plane *7*. Either a luminescent glass or a photoresist is placed here. In the first case, the image can be seen by means of microscope *8*. An objective *2* is mounted on the positioning stage in order to get a precise image projecting onto the photoresist or luminescent glass. The positioning stage allows one to translate the objective along any of three directions. If the system projects a negative image, the mask is mounted together with the objective *2* and is translated simultaneously with the objective.

For the given scheme of the experiment an estimation of the maximal variation of the transparent dimensions can be made. To estimate δf_1 let us use the thin lens approximation. Taking the logarithmic derivative of the thin lens formula, we obtain $\delta f/f = -\delta n(n-1)^{-1}$. We shall take the refraction index for small wavelengths from the Tables, e.g., [9]: $n \simeq 1.54$. To estimate δn_λ we shall use the formula $\delta n_\lambda = 0.046 \cdot 2\lambda\delta\lambda(\lambda^2 - 0.28)^{-2}$. Omitting some transformations, we obtain for the estimate $\delta f_1 = 3.22 \cdot 10^{-6}$ μm. If we count $\Delta\nu = 0.048$ cm^{-1} for $\lambda = 312.2$ nm [6], then for $\delta\lambda$, we have $\simeq 0.4 \cdot 10^{-6}\mu$m. Taking into account the values of f_1 and f_2, we obtain $\delta L \simeq 7.37 \cdot 10^{-2}\mu$m. From here it follows that the variation of the transparent dimension for the transparent with length $2l = 0.1$ m due to the finite laser emission line width under the given parameters (taking also into account the diffraction losses) can be (in accordance with (6)) up to $2\delta L = 0.147$ μm under a total system magnification of $V = 0.395$. The focal distance is changed by $3.22 \cdot 10^{-6}$ fraction of its value. Thus, the finite laser emission line width does not prevent image transfer with submicron precision.

The possibility of obtaining a sufficient UV-emission power in the projection regime is another principal

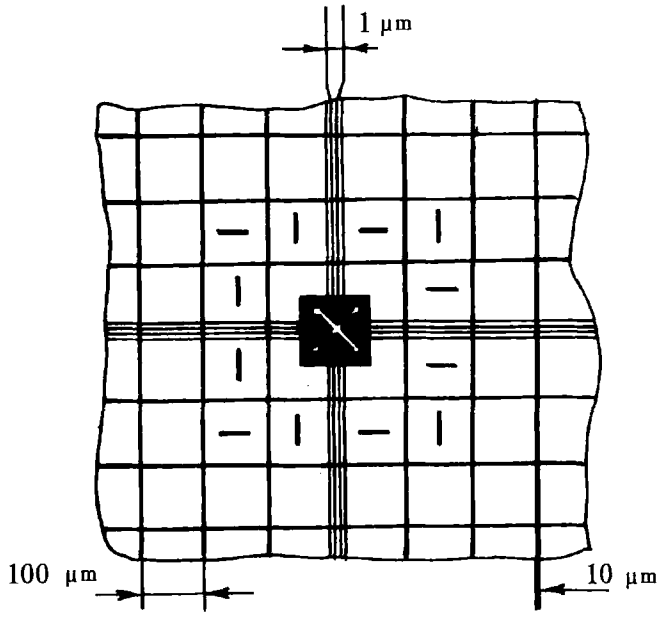

Figure 5. Photo mask.

feature. This regime is equivalent to the regime of lasing with one mirror; the latter, in turn, has different reflectivity, depending on the projection regime. Two photo masks were used in the experiments. Let us agree to consider as positive the first one, in which the dark fringes are drawn (see Fig. 5), and as negative we take the second one, in which the light transparent fringes are etched on a dark background. The dark background is Cr coating on a quartz substrate. The best image quality was realized for the positive photo mask in the shadow regime. In this case UV-emission power on the screen reached 50 – 70% of the output power of the laser with two mirrors for the tube with diameter $D_1 = 2$ cm, and 30 – 40% for the tube with diameter $D_2 = 2.7$ cm. The worsening of the quality in other cases is explained by the low transmittance of the negative photo mask in the shadow regime or by the considerable reflectivity of the pure quartz plate surface in both kinds of projection. Thus, the main experimental results were obtained with a positive photo mask in the shadow regime. During the experiment a number of features were discovered which are characteristic for the transfer of micron structures on the photo resist.

1. Since the plate to which the photo resist was applied has reflectivity, it is necessary to mount it on the adjustment assembly in order to remove the reflected beam from the optical path. To mount the photoresist at an angle, for this purpose it was necessary to enlarge the distance between the mirror *6* and plate *7* in order to diminish the inclination of plate *7* with respect to the optical axis. A satisfactory quality of the image was obtained at a focal length $f = 0.5$ m. To diminish the inclination of plate *7* the minimal possible diameter of mirror *6* was chosen so that the emission from the amplifier would fill the total mirror surface.

2. To conserve the image contrast range a part of the lens surfaces was substituted by the mirror ones, and this is natural because the aberrations are less in this case. All the surfaces of the optical elements were manufactured with precision not worse than $\Delta = \lambda/20$.

3. To avoid mechanical vibrations and air turbulence along the optical path, all the components were mounted on hard supports, and the spacings between them were carefully enclosed by tubes and caps.

4. Optimal results on the image sharpness were obtained under a 2–5-time scale-down. The same result was obtained by a theoretical estimate under chosen focal distances and optical system dimensions, $V = 0.395$.

The measures taken for the experiment optimization made it possible to distinguish easily the photo mask lines with a thickness of 1 μm in the projection microscope regime under a 1-m linear dimension of the screen and $f = 5$ cm objective. The pattern was unstable because of noneliminated turbulence flows. Thus, a system with large focal length which resolved 5-mm lines was used in the demonstration experiments. When a 2–2.5-times-reduced image was projected onto a luminescent uranile glass with the help of an available microscope, it was possible to distinguish with contrast photo mask lines with a width of 10 μm. A non-resolved dark line is seen at the location of the line with a width of 1 μm.

To estimate the real resolution power of the system, the photo mask image was projected onto a glass plate with 0.8 μm thickness positive photoresist FP-051. It was observed that the width of lines on the photoresist is noticeably wider than the lines seen on the luminescent glass. Evidently, the reason is as follows: the influence of mechanical vibrations and turbulence is masked in the projection microscope regime, but is manifested under longer exposures on the photoresist. Therefore, the exposure time was diminished as far as possible to get more contrast pictures. We have succeeded in restricting the exposure time to 10 ms by means of the laser operation control. Under such operation we have succeeded in resolving the structure of 1-μm lines. Using nonlinear photoresist sensitivity to exposure dose [1], we obtained line widths of 2 μm. This value proved to be less than the theoretical value of the ultimate resolution of the optical system used, which was estimated to be 5–6 μm.

Thus, the feasibility of micron-size image transfer and the use of the UV-emission gold-vapor laser was confirmed. Owing to the use of the nonlinear photoresist properties and the choice of the optimal exposure time, the minimal transferring fringe size proved to be even less than the one predicted by the estimation within the framework of geometrical optics approximation. This demonstrates the prospects for development and application of UV and VUV-lasers for image transfer with micron and submicron resolution in brightness amplifiers on the basis of lasers on self-terminating transitions in metal vapor. One can assume that technical improvement of the system will allow one to carry out an image transfer with characteristic dimension 0.5 μm.

References

1. W. M. Morey, *Semiconductor Lithography* (Plenum Press, N. Y.–London, 1988).
2. *Optical Systems with Brightness Amplification*, eds. B. I. Bespalov and G. A. Pasmanik [in Russian] (Institute of Applied Optics, Gorkii, 1988).
3. V. N. Borisov, A. M. Gorokhov, G. S. Evtushenko, et al., "Spatial-temporal, spectral, and energy characteristics of UV gold-vapor laser," *Kvantov. Elektron.* **18**, 1182 (1991).
4. P. A. Bokhan and V. A. Gerasimov, "Laser impulsionnel a vapeurs de substances et procede d'alimantation dudit laser," *Invention de la Republique Francaise 2529401, Ynt. Cl3: HOIS 3/22; BOPI "Bvevets - 1985"* **16**, 8354 (1985)
5. P. A. Bokhan, V. I. Silant'ev, and V. I. Solomonov, "On a mechanism limiting pulse repetition rate in copper-vapor laser," *Kvantov. Elektron.* **7**, 1264 (1980).
6. Z. G. Huang, K. Namba, and F. Shimizu, "Influence of molecular gases on the output characteristics of a copper-vapor laser," *Jpn. J. Appl. Phys.* **25**, 1677 (1986).
7. Shan Huanyan, Hon Chengyn, Wang Hong, et al., "Experimental investigation of gold-vapor laser," *Chin. J. Laser* **13**, 417 (1986).
8. A. I. Tudorovskii, *Theory of Optical Instruments*, Vols. I–II [in Russian] (Nauka, Moscow–Leningrad, 1952).

9. M. Ya. Kruger and V. A. Panov, *Handbook for Designers of Optical-Mechanical Instruments* [in Russian] (Mashinostroenie, Leningrad, 1968).
10. J. W. Goodman, *Introduction to Fourier Optics* [Russian translation] (Mir, Moscow, 1970).
11. A. Papulis, *Theory of Systems and Transformations in Optics* [Russian translation] (Mir, Moscow, 1971).
12. T. Ya. Dubnishcheva, "Shadow optical echo," in: *Holography: Theoretical and Applied Problems* [in Russian] (Leningrad, 1988) p. 172.